

Critical Dopant Concentration in Polyacetylene and Phase Diagram from a Continuous Four-Fermi Model

Heron Caldas,^{1,*} Jean-Loïc Kneur,^{2,†} Marcus Benghi Pinto,^{3,‡} and Rudnei O. Ramos^{4,§}

¹*Departamento de Ciências Naturais, Universidade Federal de São João del Rei, 36300-000, São João del Rei, MG, Brazil*

²*Laboratoire de Physique Théorique et Astroparticules - CNRS - UMR5207 Université Montpellier II, France*

³*Departamento de Física, Universidade Federal de Santa Catarina, 88040-900 Florianópolis, SC, Brazil*

⁴*Departamento de Física Teórica, Universidade do Estado do Rio de Janeiro, 20550-013 Rio de Janeiro, RJ, Brazil*

The Optimized Perturbation Theory (OPT) method, at finite temperature and finite chemical potential, is applied to the field theory model for polyacetylene. The critical dopant concentration in *trans*-polyacetylene is evaluated and compared with the available experimental data and with previous calculations. The results obtained within the OPT go beyond the standard mean field (or large- N) approximation (MFA) by explicitly including finite N effects. A critical analysis of the possible theoretical prescriptions to implement and interpret these corrections to the mean field results, given the available data, is given. For typical temperatures probed in the laboratory, our results show that the critical dopant concentration is only weakly affected by thermal effects.

PACS numbers: 64.60.A-,71.30.+h,11.10.Kk

I. INTRODUCTION

About three decades ago a remarkable discovery was made that *trans*-polyacetylene $(\text{CH})_x$ doped with halogens could behave as a metal, exhibiting electrical conductivity [1]. Since then several striking features have been shown by conjugated polymers, such as electronic, optical and magnetic properties, which give these materials a wide range of applicability [2, 3, 4, 5]. Before reaching the metallic state, polyacetylene can be converted into a semiconductor, depending on the concentration of dopant, y , defined as the number of doped electrons per carbon atom. For lower dopant concentration, the conduction can be described in terms of topological excitations, such as (spinless charged) polarons, bipolarons or solitons [6]. Experiments have also shown that the observed non-metal to metal transition in polyacetylene, that typically happens when the dopant concentration is increased to a critical value, $y_c \approx 6\%$, corresponds to a first-order transition [7].

From the theoretical point of view, the role of the (self-localized) solitons in the charge-transport process is successfully described by the model Hamiltonian proposed by Su, Shrieffer, and Heeger (SSH) [8]. SSH were primarily interested in the low-energy excitations of the one-dimensional polymer. In this case, the electronic correlation length, ξ , becomes much larger than the lattice constant, a , and an effective model Hamiltonian incorporating only the electron-phonon coupling as an interaction term, and neglecting electron-electron Coulomb repulsion, was shown to be able to give a very good description of the system. To take into account electron-electron interactions, extended versions of the SSH Hamiltonian, such as Hubbard models [5, 9], have been later employed.

The continuum limit of the SSH Hamiltonian is known as the Takayama–Lin–Liu–Maki (TLM) model [10], which is a field theory with two-flavor Dirac fermions. The TLM model gives a very good approximation to the discrete SSH model provided two conditions hold: the band gap (denoted as E_{gap}) between σ electron bonding and anti-bonding states is much smaller than the π -band width (denoted as W) and the typical distance between the neighboring single-electron levels near the Fermi energy is much smaller than the gap. The first condition is automatically fulfilled for *trans*-polyacetylene, where from the typical measured values $E_{\text{gap}}/W \simeq (1.8 \text{ eV})/(10 \text{ eV}) = 0.18$ [6], while the second one is met provided the application is for a chain with a large size [11]. At the same time, in many conducting polymers the characteristic correlation length, ξ , is much larger than the lattice constant, a . These two quantities are related to E_{gap} and W by $\xi/a = W/E_{\text{gap}}$ [6].

Some authors [12] have recognized that the corresponding Lagrangian of the TLM model is analogous to a field theoretical model for fermions with quartic self-interactions in 1+1 dimensions, also known as the Gross-Neveu (GN) model [13]. It is worth recalling that the large- N , or mean-field approximation (MFA), predicts that, at $T = 0$, the GN

*Electronic address: hcaldas@ufsj.edu.br

†Electronic address: kneur@lpta.univ-montp2.fr

‡Electronic address: marcus@fsc.ufsc.br

§Electronic address: rudnei@uerj.br

model in 1+1 dimensions suffers a first-order phase transition at the critical chemical potential value, $\mu_c = \Delta_0/\sqrt{2}$, where Δ_0 is the order parameter value at $T = 0 = \mu$ [14]. Other works making use of the GN model applied to the study of the properties of polyacetylene include Refs. [15, 16]. However, to our knowledge, the issue of investigating the phase diagram and temperature effects in the dopant concentration in polyacetylene have not been addressed, in the context of the GN model, so far.

Since we can relate the dopant concentration in terms of the chemical potential, the GN model works as an analog model that can describe, in a field theory language, the non-metal to metal phase transition observed in the *trans*-(CH)_x. An early study of the transition from the (chiral symmetry broken) low-density to the (symmetry restored) high-density phase, has been performed by the authors of Ref. [17] using the GN model, by assuming fermions with $N = 2$ flavors, but considering only the leading order in a $1/N$ expansion. Despite this approximation, it was found an excellent agreement, of about 6%, between the theoretical and experimental critical doping concentration, y_c . Later, the same authors have used a mixture of the thermodynamic Bethe ansatz (TBA) and the $1/N$ expansion at the next to the leading order (NLO) to evaluate finite N corrections to μ_c [18]. Surprisingly, their NLO does not agree so well with the experimental results, deviating by about 20%. One of our main motivations in the present work is to shed some light into this rather peculiar behavior. After all, one expects that finite N corrections should improve convergence, especially in a case where $N = 2$, like it is the case in the theoretical model description of polyacetylene. With this aim we start by remarking that the critical dopant concentration, y_c , is related to the critical density, ρ_c , and the equilibrium space, a , between the x coordinates of successive *CH* groups in the undimerized structure by $y_c = \rho_c a$. However, in Ref. [18], the authors did not compute the finite N corrections to the critical density ρ_c but rather to the value of the chemical potential μ_c . Nevertheless, they concluded that, for $N = 2$, $\rho_c(N)$ should change by about 20% since it is proportional to $\mu_c(N)$, which changes by the same amount. We believe that this conclusion is not necessarily right since additional N and/or coupling (λ) dependent factors, $\mathcal{H}(\lambda, N)$, could appear when obtaining ρ by deriving the pressure with respect to μ so that $\rho_c(N)$ could be proportional to $\mathcal{H}(\lambda, N) \mu_c(N)$ where, for example, $\mathcal{H}(\lambda, N \rightarrow \infty) \rightarrow 1$ in the mean-field approximation. Second, ρ depends on parameter values such as E_{gap} and W that sets $\xi/a = W/E_{\text{gap}}$ but only the value $\xi/a \simeq 7$, which corresponds to the original SSH parameters [8] $E_{\text{gap}} = 1.4$ eV and $W = 10$ eV, was considered in Refs. [17, 18]. We must recall that the original SSH parameter values, especially the one regarding E_{gap} , have been further updated already in the Ref. [6].

Here, we shall investigate the same problem considering again the 1+1 dimensional GN model, but not restricting the analysis to the large- N approximation. On general grounds, one may eventually wonder on the relevance of going beyond the large N (or equivalently mean field) approximation in the present context, given that the equivalence between the original TLM model and the GN field theory was established strictly speaking at the mean field level: indeed, there are important phenomenological aspects and properties of the polyacetylene that are anyway not correctly described by the sole TLM (for a review on both the success and limitations of the TLM/GN equivalence see e.g. [19]). Nevertheless, it appears sensible here to push the correspondence further in this direction at least because the TLM model is effectively a two-flavor only model: since some results and techniques to go beyond large N are available, these can be expected to improve the comparison of the GN model to polyacetylene data, as we shall see later. In this work we use the method of the optimized perturbation theory (OPT) [20], which is a nonperturbative method allowing to consider corrections going beyond the large- N (or mean-field) approximation. Our aim is to obtain relations for ρ_c which include finite N corrections. For this we will reconsider Landau's free energy density for the 1+1 dimensional GN model that has been recently derived by some of the present authors in Ref. [21], where the OPT results for the phase diagram show how this method correctly improves over mean-field results, in accordance with Landau's theorem for phase transitions in one space dimensions. In the same reference one finds N dependent analytical equations for the order parameter and chemical potential which turn out to be crucial for the present application. A detailed description of how the method works can be found in Ref. [21] and references therein.

In the present application, we will indeed show that within the OPT one can obtain the critical dopant concentration, y_c , in a consistent way, producing results which are in very good agreement with the experimental values for the *trans*-(CH)_x when up-to-date parameter values are considered. For completeness however, we will examine several possible theoretical prescriptions to implement and interpret these corrections to the mean field results. More precisely, as we shall see, the corrections to the mean-field may be interpreted in different ways within the context of polyacetylene. This is due to the fact that its description in terms of the Gross-Neveu field theory model is strictly speaking only an approximation. We shall also pay attention to the non negligible experimental error on some of the relevant available data. Apart from considering finite N corrections to y_c , we also estimate how thermal effects affect this quantity.

It is worth mentioning that an extension to the 2 + 1 dimensional GN theory is straightforward and may be of use in the investigation of superconducting electrons in quasi-two-dimensional systems [22]. In connection with the 2+1 dimensional GN model, the OPT has allowed [23] to redraw its phase diagram leading to the precise location of a tricritical point in the $T - \mu$ plane and the discovery of a mixed "liquid-gas" phase that remained undetermined for almost twenty years, since the first mean-field results appeared [24]. The compatibility of the OPT and Landau's expansion for the free energy density has been shown in Ref. [25]. In the condensed matter domain, higher order

OPT results have considerably improved early applications of the same method [26] producing some of the most precise analytical values for the shift of the critical temperature, ΔT_c , of an interacting homogeneous Bose gas when compared to the ideal gas [27]. Finally, the OPT convergence has also been proved in connection with critical theories [28, 29].

As far as thermal effects in the GN model at one space dimension and the application of these results to polyacetylene are concerned, a few comments are appropriate here. We recall that due to a well known no-go theorem [30, 31, 32], for a one-dimensional system at any finite temperature we should expect no phase transition related to a discrete symmetry breaking (in this case a discrete chiral symmetry in the massless GN model considered in this work). This is due to kink-like inhomogeneous configurations [33] that come to dominate the action functional, instead of just homogeneous, constant field configurations. This is to be contrasted to the phase transition observed since long ago in the GN model in one space dimension in the mean-field, large- N approximation [14]. This result is explained by the way the thermodynamic and the mean-field approximation are performed. If the thermodynamic limit is taken before the mean-field approximation, those large nonhomogeneous fluctuations dominate and the theorem is observed. However, if the mean-field approximation is considered first, the fluctuations are suppressed, thus seem to evade the no-go theorem. Since we are here applying the GN model as an effective analog model for the polyacetylene and this is in practice a finite size system, we do not expect the theorem to be completely observed here. In fact, a phase transition at finite temperatures is indeed observed and measured in the laboratory. Nevertheless, polyacetylene is a well-known system exhibiting a rich spectrum of nontrivial fluctuations, from solitons to polaron excitations [6]. Therefore, we may expect not only homogeneous like configurations (like in the mean-field approach), but also that the inclusion of these excitations in any theoretical calculation in this model should be considered. In this context, for example in the GN field theory model, by accounting for kink-like configurations in the large- N approximation, the authors of Ref. [34] found evidence for a crystal phase that shows up in the extreme $T \sim 0$ and large μ part of the phase diagram, while the other extreme of the phase diagram, for large T and $\mu \sim 0$, seemed to remain identical to the usual large- N results for the critical temperature and tricritical points, which are well known results [14] for the GN model. In this work we will only consider homogenous vacuum backgrounds in our thermodynamical calculations applied to the polyacetylene. By comparing our results with the experimental ones we can roughly estimate the importance of soliton-like excitations in the system. From our results, we estimate that these effects are expected to be small in the context of applying the GN model as an effective analog model to describe the thermodynamics of polyacetylene at low (laboratory) temperatures.

This work is organized as follows. In Sec. II we briefly present the TLM model and its relation to a four-fermion theory, which can be identified as the GN model. In Sec. III we review the computation of the free energy for the GN model by using the OPT method. In the same section, the temperature dependent density is obtained. The gap equation is used to set up the parameter values in Sec. IV. In Sec. V we show our phase diagrams for the *trans*-polyacetylene $(CH)_x$ both in the $T - \mu$ and $T - \rho$ planes. The critical dopant density, at zero and finite temperatures, is considered in Sec. VI. Our concluding remarks are given in Sec. VII.

II. THE TAKAYAMA-LIN-LIU-MAKI AND GROSS-NEVEU MODELS

The Takayama-Lin-Liu-Maki (TLM) Hamiltonian is the continuum version for the original SSH model and it is given in terms of a fermionic field, ψ , and a scalar field, Δ , representing the coupling of the electron gas to the local value of the dimerization and it is expressed by the Hamiltonian [10]

$$H_{\text{TLM}} = \frac{1}{2\pi\hbar v_F \lambda_{\text{TLM}}} \int dx \Delta^2(x) + \sum_s \int dx \psi^\dagger(x) [-i\hbar v_F \sigma_3 \partial_x + \sigma_1 \Delta(x)] \psi(x), \quad (2.1)$$

where the sum is over the spin states, σ_i are the Pauli matrices, $v_F = k_F/m$ is the Fermi velocity and λ_{TLM} is a dimensionless coupling defined by

$$\lambda_{\text{TLM}} = \frac{2\alpha^2}{\pi t_0 K}, \quad (2.2)$$

where α is the π -electron-phonon coupling constant of the original SSH Hamiltonian, K is the elastic chain deformation constant and t_0 is the hopping parameter, which is expressed in terms of the Fermi velocity and the equilibrium space a between the x coordinates of successive CH groups in the undimerized structure as $t_0 = \hbar v_F/(2a)$.

Note from Eq. (2.1) that a nonvanishing (constant) value for Δ leads to a mass term for the fermions, thus breaking the chiral symmetry exhibited by H_{TLM} and opening an electronic energy gap in the system. The presence of a gap

prevents electrons to move to the conduction band and, thus, the system effectively behaves as a non-metal. The effect of the addition of dopants to the system is to decrease the electronic energy gap, till it vanishes at some critical dopant concentration and the system starts to behave as a metal. In general, a kinetic term for the scalar field emerges when taking the continuum limit of the SSH model. However, we consider the usual adiabatic approximation of neglecting the lattice vibrations, valid for energies for the optical-phonons (given by $\hbar\omega_0$) smaller than the gap magnitude (2Δ). In particular, for typical values found for polyacetylene [6], $2\Delta \approx 1.8$ eV and $\hbar\omega_0 \approx 0.12$ eV, this is regarded as a valid approximation.

The model described by Eq. (2.1) can easily be shown to correspond to a four-Fermi model if we eliminate the scalar field Δ from Eq. (2.1), e.g. by using its equation of motion. Then, putting the TLM model in the Lagrangian density form one obtains

$$\mathcal{L}_{\text{TLM}} = -\frac{1}{2\pi\hbar v_F \lambda_{\text{TLM}}} \Delta^2 + \psi^\dagger (i\hbar\partial_t - i\hbar v_F \gamma_5 \partial_x - \gamma_0 \Delta) \psi, \quad (2.3)$$

where we have identified $\gamma_5 = -\sigma_3$ and $\gamma_0 = \sigma_1$. Now, eliminating Δ from Eq. (2.3) upon using $\gamma_1 = i\sigma_2$, as well as the usual relations between the Dirac matrices, leads to

$$\mathcal{L}_{\text{TLM}} = \bar{\psi} (i\hbar\gamma_0\partial_t - i\hbar v_F \gamma_1 \partial_x) \psi + \frac{\lambda_{\text{GN}}}{2N} \hbar v_F (\bar{\psi}\psi)^2, \quad (2.4)$$

which is just a four-Fermi Lagrangian density corresponding to the massless GN model [13] where N is the number of fermion flavors ($N = 2$ for polyacetylene). In Eq. (2.4) we have used Eq. (2.2) to define the GN coupling as

$$\lambda_{\text{GN}} = N\pi\lambda_{\text{TLM}} = \frac{2N\alpha^2}{t_0 K}. \quad (2.5)$$

III. THE GROSS-NEVEU MODEL IN THE OPTIMIZED PERTURBATION THEORY

Let us now turn our attention to the implementation of the OPT procedure [20] (for a long, but far from complete list of references, please see also Ref. [21] and references in there) within the model Lagrangian density given by Eq. (2.4). Applying the usual OPT interpolation prescription to the *original* four-Fermi theory, Eq. (2.4), we define the interpolated theory

$$\mathcal{L}_\delta(\psi, \bar{\psi}) = \bar{\psi} (i\hbar\gamma_0\partial_t - i\hbar v_F \gamma_1 \partial_x) \psi - \eta(1 - \delta)\bar{\psi}\psi + \delta \frac{\lambda_{\text{GN}}}{2N} \hbar v_F (\bar{\psi}\psi)^2, \quad (3.1)$$

where η is an arbitrary mass parameter. It is easy to verify that at $\delta = 0$ we have a theory of free fermions, and the original theory is recovered for $\delta = 1$. Now, by re-introducing the scalar field Δ , which can be achieved by adding the quadratic term (corresponding to a Hubbard-Stratonovich transformation)

$$- \frac{\delta N}{2\hbar v_F \lambda_{\text{GN}}} \left(\Delta + \frac{\lambda_{\text{GN}}}{N} \hbar v_F \bar{\psi}\psi \right)^2, \quad (3.2)$$

to $\mathcal{L}_\delta(\psi, \bar{\psi})$, one obtains the interpolated model corresponding to the original TLM model given by Eq. (2.3),

$$\mathcal{L}_\delta = \bar{\psi} (i\hbar\gamma_0\partial_t - i\hbar v_F \gamma_1 \partial_x) \psi - \delta\Delta\bar{\psi}\psi - \eta(1 - \delta)\bar{\psi}\psi - \frac{\delta N}{2\hbar v_F \lambda_{\text{GN}}} \Delta^2. \quad (3.3)$$

Since Eq. (3.3) is the same model already studied in Ref. [21], so we do not repeat all the details related to the free energy density derivation here, where only the main steps and results relevant for our application to the polyacetylene will be presented.

Generally, the OPT method can be implemented as follows. Any physical quantity, $\Phi^{(k)}$, is *perturbatively* computed from the interpolated model, up to some finite order- k in δ , which is formally used only as a bookkeeping parameter and set to the unity at the end of calculation. But in this process any (perturbative) result at order k in the OPT remains η dependent. This arbitrary (a priori) parameter is then fixed by a variational method that then generates

nonperturbative results, in the sense that it resums to all orders a certain class of perturbative contributions through self-consistent equations. Such optimization method is known as the principle of minimal sensitivity (PMS) and amounts to require that $\Phi^{(k)}$ be evaluated at the point where it is less sensitive to this parameter. This criterion translates into the variational relation [35]

$$\left. \frac{d\Phi^{(k)}}{d\eta} \right|_{\delta=1, \eta=\bar{\eta}} = 0. \quad (3.4)$$

The optimum value $\bar{\eta}$ that satisfies Eq. (3.4) must be a function of the original parameters, including the couplings, thus generating “non-perturbative” results. In our case, we are interested in evaluating the optimized free energy at finite temperature and density for the scalar field, Δ , once the fermions have been integrated out.

A. The Optimized Free Energy Density

To order- δ , Landau’s free energy density (or effective potential, in the language of quantum field theories) was evaluated in Ref. [21] using functional and diagrammatic techniques. The result is

$$\begin{aligned} \mathcal{F}(\Delta_c, \eta, T, \mu) = & \delta \frac{N\Delta_c^2}{2\lambda_{\text{GN}}v_F\hbar} - \frac{N}{2\pi v_F\hbar} \left\{ \eta^2 \left[\frac{1}{2} + \ln \left(\frac{M}{\eta} \right) \right] + 2(kT)^2 I_1(\eta, \mu, T) \right\} \\ & + \delta \frac{N\eta(\eta - \Delta_c)}{\pi v_F\hbar} \left[\ln \left(\frac{M}{\eta} \right) - I_2(\eta, \mu, T) \right] \\ & + \delta \frac{\lambda_{\text{GN}}}{4\pi^2 v_F\hbar} \left\{ \eta^2 \left[\ln \left(\frac{M}{\eta} \right) - I_2(\eta, \mu, T) \right]^2 + (kT)^2 I_3^2(\eta, \mu, T) \right\}. \end{aligned} \quad (3.5)$$

where k is the Boltzmann constant and the functions I_1 , I_2 and I_3 are given respectively by

$$I_1(\eta, \mu, T) = \int_0^\infty dx \left\{ \ln \left[1 + e^{-\sqrt{x^2 + \eta^2/(kT)^2} - \mu/(kT)} \right] + \ln \left[1 + e^{-\sqrt{x^2 + \eta^2/(kT)^2} + \mu/(kT)} \right] \right\}, \quad (3.6)$$

$$I_2(\eta, \mu, T) = \int_0^\infty \frac{dx}{\sqrt{x^2 + \eta^2/(kT)^2}} \left[\frac{1}{e^{\sqrt{x^2 + \eta^2/(kT)^2} + \mu/(kT)} + 1} + \frac{1}{e^{\sqrt{x^2 + \eta^2/(kT)^2} - \mu/(kT)} + 1} \right], \quad (3.7)$$

and

$$I_3(\eta, \mu, T) = \sinh \left(\frac{\mu}{kT} \right) \int_0^\infty dx \frac{1}{\cosh \left(\sqrt{x^2 + \eta^2/(kT)^2} \right) + \cosh [\mu/(kT)]}. \quad (3.8)$$

In Eq. (3.5), Δ_c is a constant field configuration for the scalar field and M is an arbitrary energy scale introduced during the regularization process used to compute the appropriate momentum integrals. In the computation performed in Ref. [21], the free energy density has been renormalized using the $\overline{\text{MS}}$ scheme for dimensional regularization. We also note that Eq. (3.5), evaluated at first order in the OPT, already takes into account corrections beyond the large- N result.

By optimizing Eq. (3.5) through the PMS condition, Eq. (3.4), we obtain the optimum value, $\bar{\eta}$, for the mass parameter, which is then re-inserted back in Eq. (3.5), allowing us to compute the order parameter $\bar{\Delta}_c$ that minimizes the free energy. Using the PMS procedure we then obtain, from Eq. (3.5), the general factorized result [21]

$$\left\{ \left[\mathcal{Y}(\eta, \mu, T) + \eta \frac{d}{d\eta} \mathcal{Y}(\eta, \mu, T) \right] \left[\eta - \Delta_c + \eta \frac{\lambda_{\text{GN}}}{2\pi N} \mathcal{Y}(\eta, \mu, T) \right] + \frac{(kT)^2 \lambda_{\text{GN}}}{2\pi N} I_3(\eta, \mu, T) \frac{d}{d\eta} I_3(\eta, \mu, T) \right\} \Big|_{\eta=\bar{\eta}} = 0, \quad (3.9)$$

where we have defined the function

$$\mathcal{Y}(\eta, \mu, T) = \ln\left(\frac{M}{\eta}\right) - I_2(\eta, \mu, T). \quad (3.10)$$

Considering the λ_{GN}/N dependent solution one notices that, when $N \rightarrow \infty$ in Eq. (3.9), $\bar{\eta} = \Delta_c$ and the mean-field standard result is exactly reproduced as usual [21, 36]. For finite N , as is our interest here, $\bar{\eta}$ and Δ_c have to be found self-consistently by solving the gap equation $d\mathcal{F}/d\Delta_c = 0$ and the PMS equation $d\mathcal{F}/d\eta = 0$ [21].

B. The density at finite temperature

The thermodynamical potential (per volume) is defined as the free energy density at its minimum, $\Omega(T, \mu) = \mathcal{F}(\bar{\eta}, \bar{\Delta}_c, T, \mu)$ and the pressure follows as $P(T, \mu) = -\Omega(T, \mu)$. The density is then obtained by the usual relation $\rho = dP/d\mu$. We must also recall that $d\mathcal{F}/d\Delta_c = 0$ at $\Delta_c = \bar{\Delta}_c$, due to the gap equation, and that $d\mathcal{F}/d\eta = 0$ at $\eta = \bar{\eta}$, due to the PMS equation. Then, terms like $(d\mathcal{F}/d\Delta_c)(d\Delta_c/d\mu)$ and $(d\mathcal{F}/d\eta)(d\eta/d\mu)$ do not contribute. One then obtains

$$\begin{aligned} \rho(T, \mu) = & \frac{1}{v_F \hbar} \left[(kT)^2 \frac{N}{\pi} I_1'(\eta, \mu, T) + \eta(\eta - \Delta_c) \frac{N}{\pi} I_2'(\eta, \mu, T) \right. \\ & \left. - \frac{\lambda_{\text{GN}}}{2\pi^2} \eta^2 I_2(\eta, \mu, T) I_2'(\eta, \mu, T) - \frac{\lambda_{\text{GN}}}{2\pi^2} (kT)^2 I_3(\eta, \mu, T) I_3'(\eta, \mu, T) \right] \Big|_{\eta=\bar{\eta}, \Delta_c=\bar{\Delta}_c} \end{aligned} \quad (3.11)$$

where the primes indicate derivatives with respect to μ . This result will be considered later when we investigate thermal effects in y_c .

IV. THE GAP ENERGY AND PARAMETER SET AT $T = 0$ AND $\mu = 0$

In order to perform a numerical analysis we must fix all parameters. This can be done by considering the gap energy. In the GN language the order parameter $\bar{\Delta}_c$ is just the TLM gap parameter which, at $T = 0$ and $\mu = 0$, we denote as Δ_0 . At order- δ this quantity is given by [21]

$$\Delta_0 = M \exp\left\{ -\frac{\pi}{\lambda_{\text{GN}} \left(1 - \frac{1}{2N}\right)} \right\} \left(1 - \frac{1}{2N}\right)^{-1}, \quad (4.1)$$

where M is an arbitrary (at the moment) renormalization scale to be discussed further below. Eq. (4.1) explicitly includes corrections beyond large- N , as obtained from our OPT approach. More precisely, taking the mean-field approximation, $N \rightarrow \infty$ in Eq. (4.1) and using the relation $\lambda_{\text{GN}} = N\pi\lambda_{\text{TLM}}$, the OPT result exactly recovers the mean-field result for $N = 2$ [6],

$$\Delta_{MF} = M \exp[-1/(2\lambda_{\text{TLM}})], \quad (4.2)$$

as one expects [21, 36].

Now some remarks concerning the arbitrary energy scale, M , and more generally on the interpretation of Eq.(4.1) in the present polyacetylene context are useful. Usually, in a renormalizable quantum field theory, one can choose arbitrary value for M and λ_{GN} will run with the scale appropriately, at a given perturbative order, so that Δ_0 remains scale-invariant as dictated by the renormalization group. For the above gap equation this means that

$$\frac{1}{\lambda_{\text{GN}}(M)} = \frac{1}{\lambda_{\text{GN}}(M_0)} + \frac{\left(1 - \frac{1}{2N}\right)}{\pi} \ln\left(\frac{M}{M_0}\right), \quad (4.3)$$

where M_0 is some reference (input) scale ¹. Equations (4.1), or Eq. (4.3), indicates that $\lambda(M)$, or equivalently Δ_0 , is the only parameter to be fixed. These equations also show that $\lambda(M) \rightarrow 0$ as $\ln^{-1}(M/M_0)$ when $M \rightarrow \infty$ which is nothing else than the asymptotic freedom displayed by the GN model. However, in the polymer physics case, the interpretation is somewhat different mainly because *both* Δ_0 and the coupling λ_{GN} are measurable quantities, as we shall exploit below. Moreover in contrast to the renormalizable field theory case all quantities here are expected to be directly finite, *i.e.*, without need of renormalization due to the explicit high energy cutoff Λ provided by the π -band width, *i.e.*, $\Lambda \sim W$. While in our calculation we have used dimensional regularization and renormalization mainly for convenience, Eq.(4.1) should be interpreted as giving the *finite*, N -dependent, corrections to the large- N results, with the arbitrary scale M (originating from dimensional regularization) to be traded for an explicit cutoff: $M \equiv \Lambda$ of order $\Lambda \sim W$. Now since M is a parameter from the theory, its precise value is thus a matter of choice to some extent, as it does not need to coincide exactly with the experimental parameter W . This implies in particular that the scale M can be dealt with in alternative ways as we shall discuss next.

Consequently, we can consider different possible prescriptions for the basic parameters of the problem, given also that some data appear to have non negligible experimental uncertainties.

- i) First, in the prescription we label (I), $\lambda_{\text{GN}}(M)$ can be simply set to its phenomenological value given by

$$\lambda_{\text{GN}}(M) = \frac{8N\alpha^2}{WK}, \quad (4.4)$$

where we have used the relation $4t_0 = W$. As discussed above this implicitly defines a scale M once assuming the theoretical prediction of Eq. (4.1).

Regarding the data numerical values, we note that this has been debated for long and different set of values appeared in the literature (see e.g. Refs. [6, 8]). As far as we are aware, it appears [19] however that the present widely accepted data values are: $K = 21 \text{ eV}/\text{\AA}^2$, $\alpha = 4.1 \text{ eV}/\text{\AA}$, $2\Delta_0 = 1.4 - 1.8 \text{ eV}$ and $W \equiv 4t_0 = 10 \text{ eV}$, which are essentially the conventional SSH values [8] except for possible higher values of Δ_0 [6], which appears as the less accurately determined experimental input. Consequently, in our study we shall take this set of input but taking the two extreme values of Δ_0 , that we will call set A and B, respectively for $2\Delta_0 = 1.4 (1.8) \text{ eV}$.

Comparing thus set A and B appears to us as a very conservative way of taking into account those experimental uncertainties, although the higher value of $2\Delta_0 \sim 1.8 \text{ eV}$ appears to be much more favored in the recent literature. Since all relevant physical quantities (such as the critical density) will depend on the cutoff scale, M , as already mentioned one possible prescription is to use Eq. (4.1) to fix the cutoff M value for given $\lambda_{\text{GN}}(M) = 8N\alpha^2/(WK)$ and Δ_0 within accuracy, *i.e.*, for each data set A and B. Eq. (4.1) shows that due to the presence of N dependent constant term $1 - 1/(2N)$, the OPT and the MFA will predict in this way different M values even when using the same set of input data parameters.

- ii) Another possible prescription, that we dub (II), is to set $M = W$ exactly, cutting off the spectrum at an energy scale of $-W/2$ [6, 19]. In such case $\lambda_{\text{GN}}(M = W)$ does not exactly match the experimental value as predicted by Eq. (4.3). Most previous authors appear to haven chosen this prescription, *i.e.*, changing the coupling λ_{GN} value in order that the mean field model best fits the polyacetylene data. We find however equally motivated to use the first interpretation since, as already mentioned, the polyacetylene data provides us with a rather precise λ_{GN} value, while there is some intrinsic arbitrariness in the precise cutoff scale value (equivalently in this case, Δ_0 fixes the energy cutoff scale M within some accuracy) ². Actually the two prescription are not fundamentally different: in the first one uses the arbitrariness of the cutoff to fit the data Δ_0 and λ_{GN} , while in the second one forces the coupling to fit the two scales Δ_0 and W , but this is essentially translating the arbitrariness of the scale inside the exponential of Eq. (4.1).
- iii) Finally let us consider yet another possible prescription (or rather interpretation) of the GN model/polyacetylene data connexion. It will define our prescription III. Namely, bearing in mind that the

¹ Note that the N -dependence of the running coupling as dictated by Eq. (4.3) differs from the standard RG one, which (at one-loop order) has a coefficient given by $1 - 1/N$ instead of $1 - 1/(2N)$. This difference is a result of OPT which modifies standard one-loop order results, in a way expected to improve the latter.

² Note also that Eq. (4.3) also allows for any other intermediate prescriptions in which $M \neq W$ and $\lambda_{\text{GN}}(M) \neq 8N\alpha^2/(WK)$, but the simultaneous equalities for these quantities is excluded because of the $2\Delta_0 = 1.4 - 1.8 \text{ eV}$ values.

equivalence between the original TLM and continuous GN model was strictly established only at the mean field theory level, we may redefine our OPT corrections in the framework of an *effective* mean field (EMF) GN description: more precisely, the OPT-modified gap energy Eq. (4.1) can be fitted by the corresponding mean field expression Eq. (4.2) provided that ones redefines “effective” mean field coupling³ λ_{EMF}^* and cutoff W_{EMF}^* :

$$\lambda_{EMF}^* \equiv \lambda_{GN} \left(1 - \frac{1}{2N} \right), \quad W_{EMF}^* \equiv M \left(1 - \frac{1}{2N} \right)^{-1}, \quad (4.5)$$

together with the identification of these effective parameters to the measured data.

This freedom of prescriptions, as discriminated above as prescriptions I, II and III, actually reflects that neither the MFA nor the OPT-improved expression of the gap energy are expected to be exact results. If available, an exact, truly non-perturbative calculation of the gap energy would be expected to fit nicely the three independent experimental measurements, t_0 (equivalently W), Δ_0 , and λ_{GN} (of course up to limited experimental accuracy). Therefore for completeness and comparison purpose, we will consider in the numerical results all these prescriptions together with data sets A and B. A summary of the different M and λ_{GN} values for each prescription and data set is given in Table I.

Inspection of Table I indeed indicates rather different values of the “bare” coupling λ_{GN} for the three prescriptions, which is essentially due to the large uncertainty in Δ_0 between sets A and B. One should not conclude from this that our description is lacking prediction. In fact, as we shall see later, the predictions for our main result on the critical dopant estimate are not strongly dependent on the coupling values, and will be only slightly different for the three cases (provided one uses the same experimental data input). Again, the most important variation will be due to the large uncertainty on Δ_0 .

	I.A	I.B	II.A	II.B	III.A	III.B
$\lambda_{GN}^{\text{OPT}}$	1.28	1.28	1.42	1.55	1.89	2.07
$\lambda_{GN}^{\text{MFA}}$	1.28	1.28	1.18	1.30	1.18	1.30
M^{OPT} (eV)	13.85	17.80	10	10	7.5	7.5
M^{MFA} (eV)	8.15	10.47	10	10	10	10

TABLE I: The OPT and MFA values for λ_{GN} and M obtained, from the gap equation, for parameter sets A ($2\Delta_0 = 1.4$ eV) and B ($2\Delta_0 = 1.8$ eV), using prescriptions I–III for fixing the relevant parameters of the model. The common values for both cases are: $K = 21$ eV/ \AA^2 , $\alpha = 4.1$ eV/ \AA and $W \equiv 4t_0 = 10$ eV.

V. PHASE DIAGRAMS

Having set the parameters for different prescriptions we can investigate the phase diagrams for the theory. Let us start by locating the second order and first order transition lines in the $T - \mu$ plane. This is shown in Fig. 1 for the choice of prescription IB. It shows the appearance of a tricritical point around $kT/M \simeq 0.012$ and $\mu/M \simeq 0.025$. Those numbers would slightly change for the other prescriptions, with the overall behavior qualitatively very similar. Although the appearance of a tricritical point is an interesting issue when considering the GN as a toy model for QCD, it has no practical implications for the polyacetylene, in which case one is concerned with temperatures lower than about $T_d \sim 400$ K, above which the polyacetylene is unstable and decomposes when heated (instead of melting) [37], that is $kT_d/M \approx 0.0020$ for $M \approx 17.80$ eV (prescription IB). This type of phase diagram has been extensively studied in Ref. [21], where analytical expressions for T_c , μ_c , as well as useful relations among tricritical points relations can be found.

As emphasized in the introduction, one of our goals here regards the evaluation of the critical concentration, y_c , as a function of the temperature. With that aim one benefits from analyzing the phase diagram in the $T - \rho$ plane since $y_c(T)$ is directly proportional to $\rho_c(T)$. This is shown in Fig. 2. The dot in Fig. 2 indicates the tricritical point above which the transition is of the second kind. The mixed (semi conductor) region is associated to the

³ Note that the meaning of effective coupling here is purely phenomenological, as obtained from a fit, and thus unrelated to the usual effective coupling $\lambda_{GN}(M)$ as above discussed having the RG behavior.

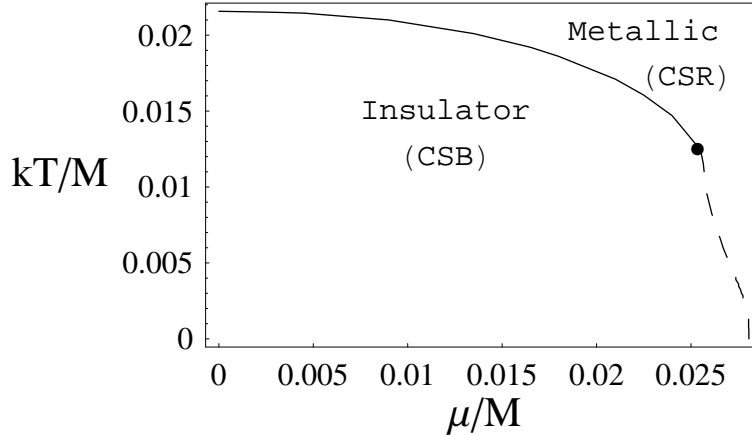


FIG. 1: The OPT phase diagram, in the kT/M - μ/M plane, for $N = 2$ and $\lambda = 1.28$ (prescriptions IA and IB in Table I). The continuous line represents the second order transition whereas the dashed line represents the first order transition and the dot indicates the tricritical point, which occurs at $kT/M \simeq 0.012$ and $\mu/M \simeq 0.025$.

first order phase transition. At $T = 0$ the critical dopant density is approximately $\rho_c(0) \simeq 0.016 M/(v_F \hbar)$. Figure 2 shows the situation where the first order transition line, which appears in the $T - \mu$ plane, splits into two lines limiting a coexistence, mixed (semiconducting) region. We note that there are indeed experimental indications of a mixed phase for polyacetylene for concentrations below the critical one [38]. It is also interesting to note, from the same figure, that when one evaluates y_c at $T = 0$ using the GN model [17, 18] the only observed transition is from the semiconducting phase to the metallic one. However, even at room temperature (roughly $kT/M \approx 0.0015$) our figure displays another transition from the (unsymmetric) insulator phase to the (mixed) semiconductor phase which happens at a rather very small density, of the order $v_F \hbar \rho/M \sim 10^{-5}$. For this transition the critical density increases with the temperature. On the other hand, the critical density when going from the (mixed) semiconducting phase to the (symmetric) metallic one seems to slightly decrease for low values of T . Figure 2 also shows that above $\rho_c(0)$, computed in the next section, the material is a conductor at any temperature, provided that this temperature is smaller than the degradation temperature, T_d . In the next section we shall devote especial attention to this issue, since the literature does not seem to indicate any previous studies of the influence of thermal effects in y_c within the models considered here.

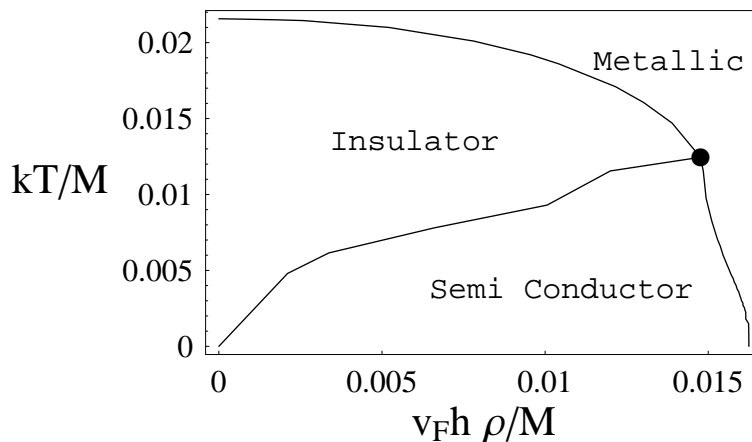


FIG. 2: The OPT phase diagram in the $kT/M - v_F \hbar \rho/M$ plane for $N = 2$ and $\lambda = 1.28$ (prescriptions IA and IB in Table I). The insulator region is associated with the unsymmetric (dimerized) phase, while the metallic region is associated with the symmetric (undimerized) phase.

VI. CRITICAL DOPANT DENSITY

In this section we evaluate the critical dopant concentration, y_c , which, with periodic boundary conditions in the polyacetylene chain, is given simply as $y_c = a\rho_c$. In the next subsection we consider the case $T = 0$ performing a numerical comparison between the MFA and the OPT using the different sets of parameters presented earlier. Next, we will consider how the temperature affects y_c .

A. The zero temperature case

In this section we will evaluate the dopant critical density in polyacetylene within the OPT approach, neglecting eventual temperature effects which will be considered in the next subsection. Let us start by taking the limit $T \rightarrow 0$ in the free energy density, Eq. (3.5). The various functions defined by Eqs. (3.6), (3.7) and (3.8), in the $T \rightarrow 0$ limit become

$$\lim_{T \rightarrow 0} (kT)^2 I_1(\eta, \mu, T) = -\frac{1}{2}\theta(\mu - \eta) \left[\eta^2 \ln \left(\frac{\mu + \sqrt{\mu^2 - \eta^2}}{\eta} \right) - \mu\sqrt{\mu^2 - \eta^2} \right], \quad (6.1)$$

$$\lim_{T \rightarrow 0} I_2(\eta, \mu, T) = \theta(\mu - \eta) \ln \left(\frac{\mu + \sqrt{\mu^2 - \eta^2}}{\eta} \right), \quad (6.2)$$

$$\lim_{T \rightarrow 0} kT I_3(\eta, \mu, T) = \text{sgn}(\mu)\theta(\mu - \eta)\sqrt{\mu^2 - \eta^2}. \quad (6.3)$$

Using Eqs. (6.1), (6.2) and (6.3) in Landau's free energy density, Eq. (3.5), we notice that it can be divided into two cases: i) $\mu < \eta$ and ii) $\mu > \eta$. At zero temperature the critical chemical potential, $\mu_c(0)$, is defined as the one which produces the same pressure for both, $\bar{\Delta}_c = \Delta_0 \neq 0$ and $\bar{\Delta}_c = 0$. This quantity, which has been evaluated in Ref. [21], is given by

$$\mu_c(0) = \frac{M}{\sqrt{2}} \exp \left\{ -\frac{\pi}{\lambda_{\text{GN}} \left(1 - \frac{1}{2N}\right)} \right\} \left(1 - \frac{\lambda_{\text{GN}}}{2\pi N}\right)^{-1/2}. \quad (6.4)$$

As expected, there are two values of ρ corresponding to $\mu_c(0)$. The first is simply $\rho = 0$, corresponding to the minimum of the free energy density that occurs at $\bar{\Delta}_c = \Delta_0 \neq 0$ for the case $\mu < \eta$ (corresponding to the $T = \mu = 0$ situation). In the second case ($\mu > \eta$), the minimum of the free energy density occurs at the origin, $\bar{\Delta}_c = 0$. In this case the PMS relation, Eq. (3.9), implies that $\bar{\eta} = 0$ and one gets, from Eq. (3.11) and after simple algebra, the result

$$\rho_c(0) = \frac{\mu_c(0)N}{\pi\hbar v_F} \left(1 - \frac{\lambda_{\text{GN}}}{2\pi N}\right), \quad (6.5)$$

where the multiplicative factor in the RHS of the above equation, $\mu_c(0)N/(\pi\hbar v_F)$, is just the MFA result (with $N = 2$). In Eq. (6.5) the term $\lambda_{\text{GN}}/(2\pi N)$ gives the first order OPT finite N corrections to $\rho_c(0)$. One can now insert Eq. (6.4) into Eq. (6.5). Using also the expression for Δ_0 , Eq. (4.1), we obtain an analytical expression for the critical density that includes finite N corrections,

$$y_c(0) = a\rho_c(0) = \frac{\sqrt{2}N\Delta_0}{\pi W} \left(1 - \frac{\lambda_{\text{GN}}}{2\pi N}\right)^{1/2} \left(1 - \frac{1}{2N}\right), \quad (6.6)$$

where we have used the defining relation $a/(\hbar v_F) = 2/W$. Note that the explicit (overall) scale M dependence disappears from Eq. (6.6), where only the physical parameters W/Δ_0 set the overall scale. However, there is an implicit scale dependence in the OPT case via the dependence on $\lambda_{\text{GN}}(M)$ within the factor $[1 - \lambda_{\text{GN}}/(2\pi N)]^{1/2}$ ⁴.

⁴ Note, however, that since $[1 - \lambda_{\text{GN}}/(2\pi N)]^{1/2} [1 - 1/(2N)] \rightarrow 1$, as $N \rightarrow \infty$, the MFA results only depend on the ratio $2\Delta_0/W = E_{\text{gap}}/W = a/\xi$.

	I.A	I.B	II.A	II.B	III.A	III.B
y_c^{OPT}	0.0448	0.0576	0.0450	0.0569	0.058	0.074
y_c^{MFA}	0.0630	0.081	0.0630	0.081	0.0630	0.081
ξ/a	7.143	5.555	7.143	5.555	7.143	5.555

TABLE II: The critical dopant concentration y_c obtained with the OPT and the MFA obtained from each of the three different prescriptions and two data sets at $T = 0$. For reference we also show the relevant values of ξ/a in each case.

Concerning our third prescription, the “effective mean field” (EMF) prescription III defined in Sec. IV, where the OPT corrections are reinterpreted differently as redefining effective coupling and scale, the corresponding expression of the critical dopant concentration is straightforward to derive using definitions Eq. (4.5) and reads:

$$y_c^{EMF}(0) = \frac{\sqrt{2}N\Delta_0}{\pi W_{EMF}^*} \left[1 - \frac{\lambda_{EMF}^*}{2\pi N \left(1 - \frac{1}{2N}\right)} \right]^{1/2}, \quad (6.7)$$

where it is again understood that corresponding set A or B data values should be used now for λ_{EMF}^* and W_{EMF}^* .

We are now in position to make predictions concerning the observable $y_c(0)$ using, for completeness, the two different sets of data parameter and our three different theoretical prescriptions. The comparison between the OPT and MFA results is shown in Table II.

As one can see from Table II, the results depend rather substantially on the experimental data set choice, due essentially to the (linear) dependence on Δ_0 . The most quoted experimental value of y_c is $y_c \sim 0.06$, although its precise value is not very accurately determined. Typically, looking e.g. at the data from Refs. [7, 39], one may infer non negligible uncertainties on the exact transition value, of about $\Delta y_c \sim 0.01$. Also, slightly higher values of y_c have been reported in other studies [40]. In contrast, the two different prescriptions I and II regarding the scale dependence only affect mildly the y_c values in the OPT case, *i.e.*, the arbitrary scale dependence, which appears only indirectly within the factor $[1 - \lambda_{GN}/(2\pi N)]$, which appears in our previous expressions like Eq. (6.6), remains moderate.

Inspection of Table II indicates that the OPT performs better for smaller values of ξ/a . We have carried out numerical simulations that indicate that, in fact, the OPT and MFA predict similar deviations from the experimental value, $y_c = 0.06$, for $\xi/a \simeq 6.4$. For $\xi/a < 6.4$, however, the OPT predictions are better than the MFA ones and the situations gets reversed for $\xi/a > 6.4$ as Table II shows. To illustrate this point we present Fig. 3, where $y_c(0)$ is plotted as a function of ξ/a , using prescription IB (Table I). This figure shows that for the value $\xi/a = 6$, which Ref. [19] refers to, the OPT ($y_c = 0.0535$) performs better than the MFA ($y_c = 0.0750$). We also remark that the same pattern is obtained when one considers others sets of values and prescriptions.

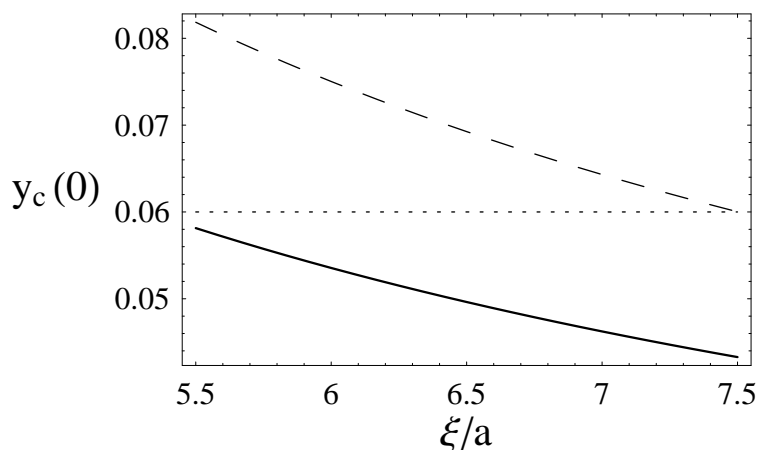


FIG. 3: The OPT (continuous line) and MFA (dashed line) predictions for $y_c(0)$ as a function of ξ/a , using prescription IB (Table I), in the relevant range $5.5 \leq \xi/a \leq 7.5$. The experimental value is $y_c(0) \simeq 0.06$.

Finally, as far the different prescriptions are concerned, we note that the ones that make use of the band gap energy as 1.8 eV (used in our data sets B in Table I), produces results with much better agreement with the experimental

data for the OPT than the MFA, as one can check from the results in Table II. In fact, this value for the band gap energy appears in the literature as a more satisfactory value for polyacetylene [6].

B. The Finite Temperature Case

To obtain the temperature dependence of the critical dopant concentration one can proceed numerically considering $y_c(T) = a\rho_c(T)$. First, as already emphasized, one should note that in practice there is an upper temperature of about $T_d \sim 400K$ above which our simple models break down since the polymer undergoes other phase transitions. Figure 4 shows that from the absolute zero temperature to the upper temperature our prediction to the decrease in the critical dopant concentration is only about 1%, while it is less than 0.5% from room temperature (about $300K$), where most of the experiments are done, to the upper temperature. This shows that in practice, at least with the type of models considered here, one may safely evaluate y_c at $T = 0$ as it has been done in Refs. [17, 18].

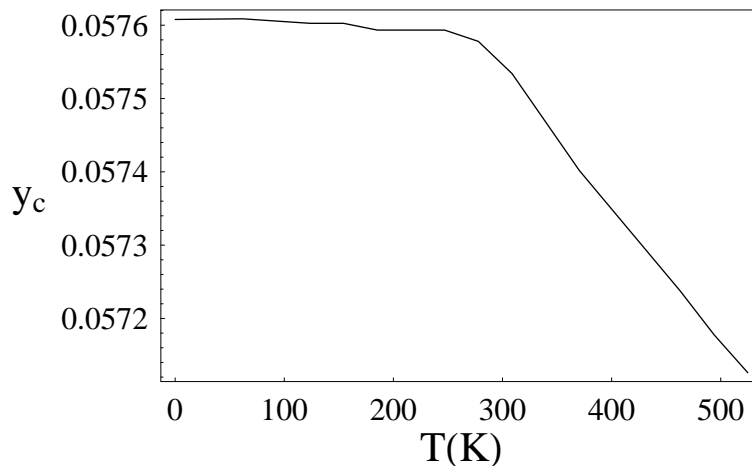


FIG. 4: The critical dopant concentration, $y_c(T)$, temperature dependence for parameters set B and procedure I. The degradation temperature is about $T_d \approx 400K$.

VII. CONCLUSIONS

Using the OPT we have reviewed the evaluation of Landau's free energy for the 1+1 dimensional massless Gross-Neveu model at finite temperature and chemical potential as performed in Ref. [21]. Then, relating this model to the TLM continuous model for polyacetylene, we have computed the critical dopant concentration, y_c , for the transition to the metallic phase. The (divergent) free energy density has been rendered finite by using a renormalization procedure which is standard in quantum field theories (\overline{MS} scheme with dimensional regularization). An arbitrary energy scale, M , introduced during the formal regularization process was fixed by using polyacetylene experimental inputs. Regarding the matching of the theory parameters to the experimental data values, we have provided a critical discussion of the possible different prescriptions to relate them giving, at the same time, the expected results for each of the prescriptions used.

The OPT formalism allows for the inclusion of finite N corrections already at the first non trivial order which should improve the usual MFA results since, for this particular case, $N = 2$. To illustrate the possible phase transitions allowed by the GN model we have obtained phase diagrams in the $T - \mu$ as well as in the $T - \rho$ planes. Then, we have obtained a neat analytical expression for $y_c = a\rho_c$ at $T = 0$ which contains explicit $1/N$ corrections. Our results show that when one uses up-to-date parameter values, the OPT results improve over the MFA as expected and are in good agreement with the experimental result. Another result of the present work regards the study of possible thermal effects in y_c . Our analysis has been performed in a numerical fashion, showing that, for a realistic temperature range, $0 < T < 400 K$, thermal effects induce a negligible decrease of y_c when going from the (mixed) semiconducting phase to the (symmetric) metallic phase.

Regarding the metal-insulator transition, one must recall the importance of the transport property and the localization problem [41, 42]. As far as polymers are concerned, it is known that their transport properties result from

the mechanism of hopping [42], which leads the conductivity to increase with the temperature till some maximum value. At the same time, disorder in the system can result in the localization of states and, if it is too strong, it can lead to an insulator behavior. The metal-insulator transition in real systems is then a consequence of the interplay of the amount of disorder, doping and the thermal activation process. On the theoretical side, an interesting possibility of extending the field theory application method we used to study the metal-insulator transition in polyacetylene, would be the calculation of the conductivity σ and the determination of its T, μ dependence. This would then allow a closer comparison with the experimental measures on this quantity. Basically, from response theory, the conductivity can be computed from a Green-Kubo formula, which entails a calculation of specific correlation functions and higher loop Feynman diagram contributions in the GN model we used. Although the calculation of σ in this context has been already considered within other approaches and approximations in the literature, we hope to pursue a detailed calculation of $\sigma(T, \mu, N)$ including finite N corrections, which we believe has not been done up to now. However, this is a non trivial calculation which is well beyond the scope of the present paper. We intend to address this issue in the future. Another interesting possible extension of the present work would be to use the OPT and the methods developed in Ref. [34] to consider the massive GN model, which can be related to the *cis*-polyacetylene.

Acknowledgments

H.C., M.B.P., and R.O.R. are partially supported by CNPq-Brazil. H.C. also thanks FAPEMIG for partial support. We are grateful to Prof. A. Heeger for a private communication regarding the experimental values of polyacetylene. We thank V. Mano for helpful information on thermal properties of polyacetylene and M. Thies for sending us an important reference.

-
- [1] H. Shirakawa, E. J. Louis, A. G. MacDiarmid, C. K. Chiang and A. J. Heeger, J. Chem. Soc., Chem. Commun., 578, 1977.
 - [2] J. H. Burroughes, C. A. Jones and R. H. Friend, Nature **335**, 137, (1988).
 - [3] Y. Yu, M. Nakano and T. Ikeda, Nature **425**, 145 (2003).
 - [4] S. Kubatkin, A. Danilov, M. Hjort, J. Cornil, J.-L. Bredas, N. Stuhr-Hansen, P. Hedega, and T. Bjrnholm, Nature **425**, 698 (2003).
 - [5] X. Lin, J. Li and S. Yip, Phys. Rev. Lett. **95**, 198303 (2005).
 - [6] A. J. Heeger, S. Kivelson, J. R. Schrieffer and W. P. Su, Rev. Mod. Phys. **60**, 781 (1988).
 - [7] J. Chen, T. -C. Chung, F. Moraes and A. J. Heeger, Solid State Commun. **53**, 757 (1985); F. Moraes, J. Chen, T. -C. Chung and A. J. Heeger, Synth. Met. **11**, 271 (1985).
 - [8] W. P. Su, J. R. Schrieffer and A. J. Heeger, Phys. Rev. Lett. **42**, 1698 (1979); Phys. Rev. B **22**, 2099 (1980).
 - [9] See, for example, X. Lin, J. Li, C. J. Forst and S. Yip, PNAS, **103**, 8943 (2006).
 - [10] H. Takayama, Y.R. Lin-Liu and K. Maki, Phys. Rev. B **21**, 2388 (1980).
 - [11] M. Mostovoy and J. Knoester, Phys. Rev. B **53**, 12057 (1996).
 - [12] S. A. Brazoviskii and N. N. Kirove, JETP Lett. **33**, 4 (1981); Pis'ma ZhETF **33**, 6 (1981); D. K. Campbell and A. R. Bishop, Phys. Rev. **B24**, 4859 (1981); Nucl. Phys. **B200**, 297 (1982).
 - [13] D. Gross and A. Neveu, Phys. Rev. D **10**, 3235 (1974).
 - [14] U. Wolff, Phys. Lett. **B157**, 303 (1985).
 - [15] E. Fradkin and J. E. Hirsch, Phys. Rev. B **27**, 1680 (1983).
 - [16] A. Saxena and A. R. Bishop, Phys. Rev. A **44**, 2251 (1991).
 - [17] A. Chodos and H. Minakata, Phys. Lett. **A191**, 39 (1994).
 - [18] A. Chodos and H. Minakata, Nucl. Phys. **B490**, 687 (1997).
 - [19] D. K. Campbell, Synt. Metals **125**, 117 (2002).
 - [20] A. Okopinska, Phys. Rev. D **35**, 1835 (1987); M. Moshe and A. Duncan, Phys. Lett. **B215**, 352 (1988).
 - [21] J.-L. Kneur, M. B. Pinto and R. O. Ramos, Phys. Rev. D **74**, 125020 (2006); Braz. J. Phys. **37**, 258 (2007).
 - [22] E. C. Marino, Lizardo and H. C. M. Nunes, Nucl. Phys. **B741**, 404 (2006), and references therein.
 - [23] J.-L. Kneur, M. B. Pinto, R. O. Ramos and E. Staudt, Phys. Rev. D **76**, 045020 (2007).
 - [24] K. G. Klimenko, Z. Phys. **C37**, 457 (1988); B. Rosenstein, S. H. Park and B. J. Warr, Phys. Rev. D **39**, 3088 (1989); Phys. Rev. Lett. **62**, 1433 (1989).
 - [25] J.-L. Kneur, M. B. Pinto, R. O. Ramos and E. Staudt, Phys. Lett. **B657**, 136 (2007).
 - [26] F. F. Souza Cruz, M. B. Pinto and R. O. Ramos, Phys. Rev. B **64**, 014515 (2001); Laser Phys. **12**, 203 (2002).
 - [27] J.-L. Kneur, A. Neveu and M. B. Pinto, Phys. Rev. A **69**, 053624 (2004), J.-L. Kneur and M. B. Pinto, Phys. Rev. A **71**, 033613 (2005); B. Kastening, Phys. Rev. A **70**, 043621 (2004).
 - [28] J.-L. Kneur, M. B. Pinto and R. O. Ramos, Phys. Rev. Lett. **89**, 210403 (2002); Phys. Rev. **A68**, 043615 (2003).
 - [29] E. Braaten and E. Radescu, Phys. Rev. Lett. **89**, 271602 (2002); Phys. Rev. **A66**, 063601 (2002).
 - [30] L. D. Landau and E. M. Lifshitz, *Statistical Physics* (Pergamon, N.Y., 1958) p. 482.

- [31] N. D. Mermin and H. Wagner, Phys. Rev. Lett. **17**, 1133 (1966).
- [32] S. Coleman, Commun. Math. Phys. **31**, 259 (1973).
- [33] R. F. Dashen, S.-K. Ma and R. Rajaraman, Phys. Rev. D **11**, 1499 (1974); S. H. Park, B. Rosenstein and B. Warr, Phys. Rept. **205**, 108 (1991).
- [34] O. Schnetz, M. Thies and K. Urlich, Ann. Phys. (NY) **314**, 425 (2004); M. Thies and K. Urlich, Phys. Rev. D **72**, 105008 (2005); M. Thies, J. Phys. **A39**, 12707 (2006).
- [35] P. M. Stevenson, Phys. Rev. D **23**, 2961 (1981); Nucl. Phys. **B203**, 472 (1982).
- [36] S. K. Gandhi, H. F. Jones and M. B. Pinto, Nucl. Phys. **B359**, 429 (1991).
- [37] T. Anderson and S. Roth, Braz. J. Phys. **24**, 746 (1994).
- [38] L. W. Shacklette and J. E. Toth, Phys. Rev. B **32**, 5892 (1985).
- [39] T. C. Chung, F. Moraes, J. D. Flood and A. J. Heeger, Phys. Rev. B **29**, 2341 (1984).
- [40] E. M. Conwell, H. A. Mizes and S. Jeyadev, Phys. Rev. B **40**, 1630 (1989).
- [41] A. B. Kaiser, Rep. Prog. Phys. **64**, 1 (2001).
- [42] V. N. Prigodin and A. J. Epstein, Synth. Met. **125**, 43 (2002).